A Novel Cooperative HARQ Protocol for Free-Space Optical Broadcasting Systems

Seyyed Saleh Hosseini, *Student Member, IEEE*, Jamshid Abouei, *Senior Member, IEEE*, Benoit Champagne, *Senior Member, IEEE*, and Xiao-Wen Chang

***Abstract*—In this paper, we propose a new hybrid automatic repeat request (HARQ) transmission protocol for broadcasting systems over free space optical (FSO) channels, which is applicable to both incremental redundancy (IR) and chase combining (CC) schemes. In traditional optical HARQ systems, upon receiving a non-acknowledgment (NACK) signal from a given user, the corresponding data packet is retransmitted from the central node to that user. However, in the proposed transmission protocol, called *cooperative interuser retransmission protocol* (CIRP), the optical users cooperate in the ARQ process. Specifically, instead of relying on the central node, a user who successfully decoded the original data packet and whose distance from the NACK issuing user is smaller than that of the central node, is invited to retransmit this packet to the latter user. This interuser cooperation, in fact, leverages the distance-dependent scintillation effect and path loss, which critically impact FSO channels and degrade the receiver's signal-to-noise ratio (SNR) as distance increases. We provide a detailed performance analysis of both the proposed and traditional protocols in terms of the achievable average sum rate and the next round probability of success. Our numerical results demonstrate that the former outperforms the latter for both IR and CC schemes under various turbulence conditions as well as in the presence of pointing errors.**

***Index Terms*—Free-space optical (FSO) communications, hybrid automatic repeat request (HARQ), incremental redundancy, chase combining, optical broadcasting, random pointing error.**

I. Introduction

THE history of a practical free-space optical (FSO) communication system dates back to the invention of the photophone by A. Graham Bell in 1880, when a voice signal was modulated by a light beam and transmitted at a distance exceeding 200 meters [1]. Although Bell's invention was employed for military purposes during both world wars, it took a long time for its commercial potentiality to be recognized by the industry. During the last two decades, the FSO technology has received considerable attention in the terrestrial last mile communications owing to its high data rates, ease of implementation, and low power consumption, along with huge license-free bandwidth [2]–[6]. Despite the many benefits of FSO technology, several detrimental effects of the environment such as aerosol scattering, building-sway, and atmospheric turbulence-induced fading considerably affect the performance of FSO links. Among these phenomena, the optical fading and the pointing errors, arising from random perturbations of air refractive index and random building-sway, respectively, are by far the most severe impairments which limit the application of FSO communications over long distance links [7], [8].

In order to alleviate the aforementioned impairments, several research works have leveraged techniques initially developed for radio frequency (RF) transmission across FSO links [9]–[13]. For instance, it is shown in [9] that utilizing multiple transmit and receive apertures significantly improves the bit error rate (BER) performance of FSO systems. The hybrid automatic repeat request (HARQ) is another concept which has been extended and analyzed for FSO systems from both theoretical and practical perspectives in [14]–[20]. In [19], the outage probability and average transmission rates of HARQ systems with incremental redundancy (IR) [21] and chase combining (CC) [22] schemes are analyzed, and it is shown that IR outperforms CC in terms of error probability. Recently, it has been shown in [23] that the use of polar codes in multiple-input multiple-output (MIMO) FSO systems provides robustness against spatially correlated optical fading. A 3-bit encoding scheme along with double adaptive detection thresholds is introduced in [5], where it is shown to significantly improve the performance of an FSO system.

The aforementioned works have focused on point-to-point FSO communications where only one transmit aperture sends messages to one destination, either with or without relay intervention. Recently, it has been shown in [24], [25] that multiuser point-to-multipoint scheduling can be adapted to FSO channels. The performance analysis of multiuser FSO systems under various environments has been carried out in [26]–[29]. The practical implementation of an FSO broadcasting system which serves simultaneously multiple users is described in [30]. While data communication over FSO channels can benefit substantially from the use of efficient HARQ schemes, as pointed out in [14]–[17] for the single-user scenario, this critical aspects has not received significant attention in the multiuser scenario and

Manuscript received September 12, 2019; revised December 15, 2019; accepted February 1, 2020. Date of publication February 14, 2020; date of current version April 1, 2020. This work was supported by the Natural Sciences and Engineering Research Council of Canada (NSERC) under Grant RGPIN-2017-05138 and Grant RGPIN-2017-04223. *(Corresponding author: Seyyed Hosseini.)*

Seyyed Saleh Hosseini and Benoit Champagne are with the Department of Electrical and Computer Engineering, McGill University, Montreal, QC H3A 0E9, Canada (e-mail: seyyed.hosseini@mail.mcgill.ca; benoit.champagne@mcgill.ca).

Jamshid Abouei is with the Department of Electrical Engineering, Yazd University, Yazd 89195-741, Iran (e-mail: abouei@yazd.ac.ir).

Xiao-Wen Chang is with the School of Computer Science, McGill University, Montreal, QC H3A 0E9, Canada (e-mail: chang@cs.mcgill.ca).

Color versions of one or more of the figures in this article are available online at http://ieeexplore.ieee.org.

Digital Object Identifier 10.1109/JLT.2020.2973989

several key issues remain to be investigated. This fact motivates us to further study the HARQ schemes for an FSO broadcasting system and explore the possible strategies to improve the system performance under various conditions.

This paper focuses on the incorporation of two well-known HARQ schemes, i.e., IR and CC, into an FSO broadcasting system, in which the central node transmits the same information modulated light beam to a finite number of fixed users. In traditional optical HARQ systems, a data packet is retransmitted from the central node to a user, say A, upon receiving a non-acknowledgment (NACK) signal from that user. However, in our proposed transmission protocol, called *cooperative interuser retransmission protocol* (CIRP), optical users cooperate in the ARQ process. Specifically, instead of relying on the central node, another user, say B, who successfully decoded the original data packet and whose distance from the NACK issuing user A, is smaller than that of the central node, is invited to retransmit this packet to user A. This interuser cooperation, in fact, leverages the distance-dependent scintillation effect and path loss, which critically impact FSO channels and degrade the receiver's signal-to-noise ratio (SNR) as distance increases [31]. We select the maximum achievable sum rate and next round probability of success (NRPS) as the performance metrics and analyze both protocols from an information-theoretic point of view. In particular, the average sum rate maximization problem is formulated in the case of CIRP with two and three users and for the traditional protocol with any number of users, while the extension of this analysis to the general case is discussed for the CIRP. We also derive the closed-form NRPS expressions of both protocols for any number of users. With the aid of numerical analysis, we show that the CIRP outperforms its traditional counterpart in terms of achievable sum rate and NRPS under a wide range of turbulence conditions with and without random pointing errors.

The rest of the paper is organized as follows. In Section II, the system model and assumptions are described. The proposed CIRP is presented in Section III, along with an analysis of the maximum achievable average sum rate for an FSO HARQ system under both the CIRP and the traditional protocol. In Section IV, numerical results are provided to show the advantages of our proposed CIRP over the traditional protocol. Finally, conclusions are drawn in Section V.

Notation: A real Gaussian random variable z with mean μ and variance σ^2 is represented by $z \sim \mathcal{N}(\mu, \sigma^2)$. $\mathbb{E}[x]$ stands for the expectation of random variable x, while $\mathbb{P}\{.\}$ denotes the probability of a given event. The error function is defined as $\text{erf}(x) \triangleq \frac{2}{\sqrt{\pi}} \int_0^x e^{-t^2} dt$. The discrete unit step and impulse functions are represented by $u(\ell)$ and $\delta(\ell)$, respectively.

II. Broadcasting FSO System Model

In this work, we consider a broadcasting FSO system consisting of a central node and $N > 1$ fixed users. We identify the central node with index $i = 0$ and the user nodes with index $i \in \mathcal{I} = \{1, \ldots, N\}$, and we let $\mathcal{I}_0 = \mathcal{I} \cup \{0\}$ denote the complete index set. The broadcast information signals are transmitted from the central node as binary packets (or frames) of length K. A user who does not successfully receive a packet can request its retransmission by sending a NACK signal to either the central node or a nearby user, where the latter option only applies to the CIRP. The initial transmission is indexed by $\ell = 0$ while the subsequent ARQ rounds are indexed by $\ell \in \mathcal{L} = \{1, \ldots, L\}$, where L is the maximum number of rounds. The length of the transmitted packet in each round is denoted as K_ℓ: for the initial transmission, $K_0 = K$, while for subsequent ARQ rounds, the value of K_ℓ depends on the particular retransmission scheme being adopted. For both the traditional protocol and proposed CIRP, there exists a one-way optical link from the central node to user i, represented by $(i, 0)$, which is used to (re)transmit optical signals within ARQ rounds. However, a two-way optical path from user j to user i, represented by the pair (i, j), is also considered for the CIRP as further explained in Section III. It is assumed that all feedbacks from the users to the central node are implemented using separate wireless channels at radio frequencies, and are free of errors and delays. A general illustration of this setting is presented in Fig. 1.

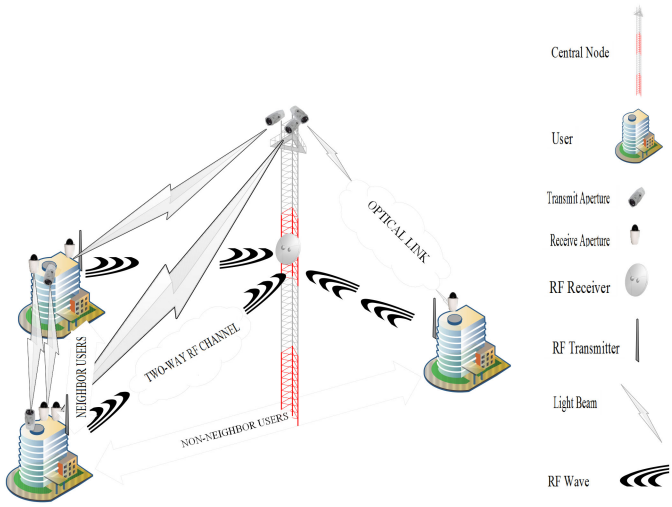

Fig. 1. A typical broadcasting FSO system operating under an HARQ protocol.

At the central node, the transmitted bits are intensity modulated using on-off keing (OOK). It is assumed that the extinction ratio of the transmitter is large enough such that the transmitted optical power can be ignored within the off period [32]. The optical links between the central node and the fixed users can support high-rate packet based transmissions ($\approx 10^9$ bps or more). The links can be assumed to be frequency-flat fading since the coherence bandwidth exceeds the communication bandwidth due to the negligible multipath spreading effect [24]. It is assumed that the coherence time of these links is greater than the required time for all possible (re)transmissions of a packet, such that the channel remain constant within $(L + 1)$ rounds and change independently in the next coherence time. [1] This scenario corresponds to the worst-case one since the time

[1] The coherence time of a flat fading point-to-point link is broadly defined as the time interval during which the channel gain of the link remains correlated (ideally constant). Once this interval is over, the channel gain may be assumed to change to a new, nearly uncorrelated value.

diversity can not be exploited to improve system performance [33].

Assuming that the direct detection is employed by the users to convert the received optical power into non-negative electrical signals, the information signal received by user i from either the central node or user j for round ℓ of the HARQ process, can be expressed as [8], [24], [34], [35]

$$y_{\ell k}^{(i,j)} = 2\rho h^{(i,j)} P_t s_{\ell k} + n_{\ell k}^{(i,j)}, i \in \mathcal{I}, j \in \mathcal{I}_0, k \in 1, \ldots, K_\ell, \tag{1}$$

where $s_{\ell k} \in \{0, 1\}$ denotes the k^{th} intensity modulated information bit within the current packet, P_t is the average optical transmission power of the OOK modulator, and $h^{(i,j)}$ is the compound channel effect, as further explained below. The parameter ρ is the photodetector's responsivity which depends on the quantum efficiency, electron charge, Planck's constant, and optical frequency. The additive term $n_{\ell k}^{(i,j)}$ represents thermal noise, modeled as a zero-mean white noise process with Gaussian distribution, i.e., $n_{\ell k}^{(i,j)} \sim \mathcal{N}(0, \sigma_n^2)$ [8], [35].

A. Compound Channel Model

In this part, the link's superscript $(.)^{(i,j)}$ is dropped for simplicity. The compound channel effect in (1) is defined as $h \triangleq h_o h_t h_p$ where h_o is the path loss of optical link, h_t is the turbulence-induced fading whose strength depends on the environmental condition, and h_p is the random pointing errors [8]. Below, we explain how these three components can be modeled for an FSO channel:

- *Path Loss:* The parameter h_o is the deterministic component of the aggregated FSO channel characterizing, the extent to which the transmission power is attenuated over an FSO link. This attenuation is caused by the Mie scattering phenomenon and can be described by the Beer-Lambert's law as $h_o \triangleq \exp(-\zeta d)$ where d is the path length and ζ is the attenuation coefficient depending upon the wavelength and visibility [36], [37].
- *Turbulence-Induced Fading:* The parameter h_t, also called random irradiance fluctuation, and is modeled as a gamma-gamma random variable with PDF [38, p. 370]:

$$f_{h_t}(h_t) = \frac{2(\alpha\beta)^{\frac{\alpha+\beta}{2}}}{\Gamma(\alpha)\Gamma(\beta)} h_t^{\frac{\alpha+\beta}{2}-1} K_{\alpha-\beta}(2\sqrt{\alpha\beta h_t}),\ h_t > 0, \tag{2}$$

where α and β are the shaping parameters of small-scale and large-scale eddies in the scattering environment, $\Gamma(x) = \int_0^\infty t^{x-1} e^{-t} dt$, and $K_\nu(.)$ denotes the modified Bessel function of the second kind of order ν. The parameters α and β are dependent on the Rytov variance σ_R^2 which is defined for the path length d as $\sigma_R^2 \triangleq 1.23 C_n^2 (\frac{2\pi}{\lambda})^{7/6} d^{11/6}$ where C_n^2 and λ are the refractive index and operating wavelength, respectively [8]. The explicit relationships between the shaping parameters α, β, and the Rytov variance σ_R^2 can be found in [38]. The normalized variance of h_t, known as *scintillation index*, plays a crucial role in the performance of an optical communication system and is defined as

$$\sigma_{h_t}^2 \triangleq \frac{\mathbb{E}[h_t^2] - \mathbb{E}^2[h_t]}{\mathbb{E}^2[h_t]} = \frac{1}{\alpha} + \frac{1}{\beta} + \frac{1}{\alpha\beta}. \tag{3}$$

- *Random Pointing Errors:* The parameter h_p, also called misalignment fading, arises from the misalignment of the transmitted light beam on the detector plane of the receiver due to the high-rise building sway [13], [39].

It is shown in [8] that the PDF of the random pointing errors can be accurately approximated by

$$f_{h_p}(h_p) = \frac{\xi}{A_0^\xi} h_p^{\xi-1},\ 0 < h_p < A_0, \tag{4}$$

where $A_0 \triangleq \text{erf}^2(v)$, $v \triangleq \sqrt{\frac{\pi}{2}} \frac{a}{\omega_d}$, and a is the detector's radius. The parameter ω_d is the beam waist at distance d, defined as $\omega_d \triangleq \omega_0 [1 + (1 + 2(\frac{\omega_0}{\rho_d})^2)(\frac{\lambda d}{\pi \omega_0^2})^2]^{\frac{1}{2}}$ where $\rho_d \triangleq (0.55 C_n^2 (\frac{2\pi}{\lambda})^2 d)^{-3/5}$ and ω_0 is the beam waist at $d = 0$. Finally, $\xi \triangleq \frac{\sqrt{\pi}}{8} \frac{\text{erf}(v)}{v \exp(-v^2)} \frac{\omega_d^2}{\sigma_{pe}^2}$ where σ_{pe} is the jitter standard deviation.

B. HARQ Retransmission Schemes

The performance of an HARQ protocol critically depends on the specific scheme adopted for the retransmission of lost or erroneous packets. Below, we review the main characteristics of the two most commonly used schemes, i.e., IR and CC.

1) Incremental Redundancy: In this HARQ scheme, each binary packet of length K is encoded into a set of $(L+1)$ incremental sub-codewords $\mathbf{c}_\ell$ with respective length K_ℓ for $\ell \in \{0, 1, \ldots, L\}$, where without loss of generality, we set $K_0 = K$. For the first transmission round, i.e., $\ell = 0$, the first sub-codeword $\mathbf{c}_0$ with length K_0 is sent to the receiver. At the receiver side, the direct detection as in (1) is utilized to convert the corresponding received sub-codeword into an electrical signal and decode its content. If the data is successfully decoded, an acknowledgment (ACK) will be fed back to the transmitter. Otherwise, a NACK signal is sent back by the receiver to request retransmission, corresponding to $\ell = 1$. In this case, the central node (or a substitute in the case of CIRP) transmits the subsequent sub-codeword $\mathbf{c}_1$ as additional information to assist the receiver in the decoding process. This procedure will be repeated until the receiver decodes successfully the transmitted packet or the maximum number of allowed retransmissions, i.e., L is reached. In the latter case, an error will be declared by the receiver. It should be noted that for each (re)transmission round ℓ, the decoding process is performed based on all received packets by the end of that round [33]. In practice, the sub-codewords are designed in an incremental way, with the aim to increase the probability of successful transmission, without the throughput requirements of a full retransmission as in CC.

2) Chase Combining: In this HARQ scheme, upon reception of a NACK, the same original packet of length K is retransmitted by the central node at each round. At the destination, the receiver utilizes a well-known method of diversity, i.e., maximum ratio combining (MRC), to achieve the optimal performance [33].

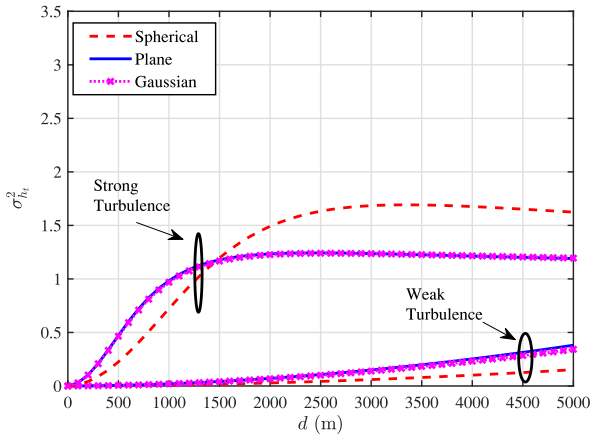

Fig. 2. Scintillation index versus distance for different types of optical waves.

III. Proposed HARQ Protocol and Performance Analysis

In this section, we first elaborate the details of the proposed HARQ transmission protocol for broadcasting in FSO channels. Subsequently, we analyze the maximum achievable sum rate for both the proposed and traditional protocols from an information-theoretic point of view.

A. Proposed Protocol

For the traditional protocol, the retransmission process is entrusted to the central node and users only confirm the correct or erroneous nature of the received packets. The users, hence, do not participate in the retransmission, even though they could effectively cooperate in this process. To shed light on this point, we first provide insight into the behavior of the scintillation index in relation to distance d. Specifically, Fig. 2 depicts $\sigma^2_{h_t}$ versus d for different types of optical waves, i.e. spherical, plane, Gaussian [38], [40]. As seen from the figure, the scintillation index is a monotonically increasing function of d when the turbulence is weak. For the strong turbulence, this trend is observed for shorter distances but with a much faster rate of increase, while for larger distances a saturation effect is noted. By considering this inherent property of FSO channels, the system performance over a shorter distance is expected to be less influenced, not only by the path loss effect, but also the turbulence-induced fading.

In an FSO broadcasting system, if there exist a pair of users with shorter distance between them than to the central node, (subsequently referred to as *neighboring users*), we could leverage these users by engaging them in the retransmission process of the HARQ protocol. To this end, we propose the CIRP, in which some users are assisted by selected neighbors in the retransmission process.

Consider a homogeneous[2] FSO broadcasting system with one central node and $N \geq 2$ users. We assume that each user is allowed to have two reception links, that is, one with the central node and one with a neighboring user, and one transmission link with another neighboring user. Therefore, each user is equipped with only one transmit and two receive apertures. The transmit aperture is directed to the receive aperture of a *neighboring user*, while the receive apertures are directed to the transmit apertures of the central node and *the same ($N = 2$) or another ($N > 2$) neighboring user*. This limitation, i.e., three apertures per user, decreases the equipment overhead and facilitates the implementation of the protocol for any number of users.

At the initial round, the central node transmits the packet corresponding to sub-codeword $\mathbf{c}_0$ to all users and then, users send back ACK or NACK signals to the central node. Consider a pair of neighboring users i and j where the receive aperture of user i is directed to the transmit aperture of user j. If both neighboring users fail to decode the packet corresponding to sub-codeword $\mathbf{c}_\ell$, the next packet corresponding to sub-codeword $\mathbf{c}_{\ell+1}$ is transmitted by the central node to both users i and j.

For this pair, if user i decodes the received packet $\mathbf{c}_\ell$ with an error while user j decodes it successfully, the central node requests user j to encode data and retransmit the packet corresponding to sub-codeword $\mathbf{c}_{\ell+1}$ to user i in the next retransmission round. The scheduling is performed by the central node which informs the users by transmitting very short messages over the RF links. Following this request, the optical transmission links between the central node and both users i and j will be disconnected from round $(\ell+1)$ on. From now on, if user i cannot still successfully decode the packet, it requests virtually the packet retransmissions from user j until L is reached. Specifically, user i makes a request again by sending a NACK signal to the central node and then, the central node requests user j to retransmit the packet to user i.

It should be noted that each user is receiving data from either the central node or only one neighboring user in each (re)transmission round for a broadcasting system with N users. Also, each user can retransmit the packets to only one neighboring user. Although more neighboring users can be utilized for retransmission procedure (as one user might have several neighboring users which are nearer than the central node), this practice implies an increase in the number of required transmit and receive apertures per user as well as more complex scheduling in the central node. In case there exist several neighboring users for a specific user, the neighboring user for creating transmission and reception link is selected based on the distance and other practical considerations.

B. Performance Analysis

In this subsection, we analyze the maximum achievable sum rate attained by an FSO broadcasting system which operates under the IR or the CC scheme. In our analysis, we assume that for a specific user there exists a neighboring user which is nearer to that user than the central node.

For the $(i,j)^{th}$ optical link, let us define the event of successful decoding at the ℓ^{th} ARQ round as

$$\mathcal{S}_\ell^{(i,j)} \triangleq \begin{cases} R_\ell^{(i,j)} < C(\gamma^{(i,j)}), & \text{for IR scheme} \\ R^{(i,j)} < C(\ell\gamma^{(i,j)}), & \text{for CC scheme} \end{cases} \tag{5}$$

where $R_\ell^{(i,j)}$ is the data rate at the ℓ^{th} (re)transmission round for the IR scheme and $R^{(i,j)}$ is the data rate of the CC scheme in all ARQ rounds. Note that we have $0 \leqslant R_\ell^{(i,j)} \leqslant R_{\ell-1}^{(i,j)} \leqslant 1$ and

[2]The FSO system is referred to as homogeneous if all users are located at the same distance from the central node.

$0 \leqslant R^{(i,j)} \leqslant 1$. In (5), $C(\gamma^{(i,j)})$ is the capacity of a discrete-time binary-input channel as a function of instantaneous SNR $\gamma^{(i,j)}$ which is defined as $\gamma^{(i,j)} \triangleq 2\rho^2(\frac{h^{(i,j)}}{\sigma_n})^2 {P_t}^2$ [8]. We denote the complementary event of $\mathcal{S}_\ell^{(i,j)}$ by $\mathcal{F}_\ell^{(i,j)}$.

Similar to [33], [41], the analysis of maximum achievable sum rate is carried out based on two information-theoretic assumptions: i) The information bits are encoded by a sufficiently long coding scheme such that the noise effect can be averaged out. Under this condition, $\mathcal{F}_\ell^{(i,j)}$ happens if the current (re)transmission rate exceeds the instantaneous channel capacity (or equivalently an outage event occurs). ii) For the $(i,j)^{th}$ optical link at two consecutive ARQ rounds, $\mathcal{S}_\ell^{(i,j)}$ should include $\mathcal{S}_{\ell-1}^{(i,j)}$. This condition, i.e., $\mathcal{S}_{\ell-1}^{(i,j)} \subset \mathcal{S}_\ell^{(i,j)}$ essentially means that the probability of successful decoding is only boosted by increasing the channel capacity or reducing the data rate in successive retransmission rounds.

1) Traditional HARQ Protocol: In this type of HARQ protocol, each user is allowed to request a packet retransmission up to L times from the central node. Hence, successful decoding can occur at one of L possible (re)transmission rounds, otherwise, an error is declared at the end of the L^{th} retransmission round, i.e., $\mathcal{F}_L^{(i,0)}$ occurs and rate of successful transmission is zero. Therefore, the successful transmission rate over the optical link $(i,0)$ is a discrete random variable which takes $(L+1)$ values and is defined as

$$\Upsilon_{\text{IR}}^{(i,0)} \triangleq \begin{cases} R_\ell^{(i,0)}, & \mathcal{S}_\ell^{(i,0)} \\ 0, & \mathcal{F}_L^{(i,0)} \end{cases} \tag{6}$$

and

$$\Upsilon_{\text{CC}}^{(i,0)} \triangleq \begin{cases} \frac{1}{\ell} R^{(i,0)}, & \mathcal{S}_\ell^{(i,0)} \\ 0, & \mathcal{F}_L^{(i,0)} \end{cases} \tag{7}$$

for the IR and the CC schemes, respectively. Moreover, we define the corresponding link success probability (LSP) of (i,j) as

$$\pi_{(m,n)}^{(i,j)} \triangleq \mathbb{P}\{R_m^{(i,j)} < C(\gamma^{(i,j)}) < R_n^{(i,j)}\}, \tag{8}$$

and

$$\kappa_{(m,n)}^{(i,j)} \triangleq \mathbb{P}\{C(m\gamma^{(i,j)}) < R^{(i,j)} < C(n\gamma^{(i,j)})\}, \tag{9}$$

for $i \neq j$ where $R_0^{(i,j)} \triangleq 1$ and $R_\infty^{(i,j)} \triangleq 0$. [3] Using these definitions along with (6) and (7), the average rate of user i can be written as

$$\overline{\Upsilon}_{\text{IR}}^{(i,0)} = \sum_{\ell=1}^{L} R_\ell^{(i,0)} \pi_{(\ell,\ell-1)}^{(i,0)}, \tag{10}$$

$$\overline{\Upsilon}_{\text{CC}}^{(i,0)} = \sum_{\ell=1}^{L} \frac{1}{\ell} R^{(i,0)} \kappa_{(\ell-1,\ell)}^{(i,0)}, \tag{11}$$

[3]Here, since the number of retransmission rounds is limited to L, the symbol ∞ should be interpreted as $L+1$.

for the IR and the CC schemes, respectively. Hence, the average sum rate can be simply obtained as follows:

$$\overline{\Upsilon}_{\text{IR}} = \sum_{i=1}^{N} \overline{\Upsilon}_{\text{IR}}^{(i,0)}, \tag{12}$$

$$\overline{\Upsilon}_{\text{CC}} = \sum_{i=1}^{N} \overline{\Upsilon}_{\text{CC}}^{(i,0)}. \tag{13}$$

As explained earlier, the main goal of this work is to maximize the average sum rate of the FSO broadcasting system which operates under the IR or CC scheme. Using (12) and (13), we formulate the optimization problems

$$\begin{aligned} &\max \overline{\Upsilon}_{\text{IR}}, \\ &\text{s.t. } 0 \leqslant R_\ell^{(i,0)} \leqslant R_{\ell-1}^{(i,0)} \leqslant 1 \text{ and } R_\ell^{(i,0)} = R_\ell^{(j,0)}, \\ &\quad i \neq j, i, j \in \mathcal{I}, \ell \in \mathcal{L}, \end{aligned} \tag{14}$$

and

$$\begin{aligned} &\max \overline{\Upsilon}_{\text{CC}}, \\ &\text{s.t. } 0 \leqslant R^{(i,0)} \leqslant 1 \text{ and } R^{(i,0)} = R^{(j,0)}, \\ &\quad i \neq j, i, j \in \mathcal{I}, \end{aligned} \tag{15}$$

for the IR and CC schemes, respectively. The second constraint in both (14) and (15) expresses that the achievable rate for each user is the same and hence, the fairness is guaranteed among all users.

Next, we aim to solve the above optimization problems. In the first step, we find a tractable expression of the channel capacity for computing $\pi_{(\ell,\ell-1)}^{(i,0)}$ and $\kappa_{(\ell,\ell-1)}^{(i,0)}$ in (10) and (11), respectively. Since there is no exact closed-form formula for the capacity of channels with finite-size input alphabet [42]–[44], we inevitably resort to using a simple exponential expression which accurately approximates the capacity as [44]

$$C(\gamma^{(i,j)}) \approx 1 - \exp(-b\gamma^{(i,j)}), \tag{16}$$

where b is a constellation-dependent constant which can be experimentally found as $b = 0.32$ for the OOK modulation. By considering (10), (11), and (16) one can rewrite the optimization problems in (14) and (15) as follows:

$$\begin{aligned} &\max \sum_{i=1}^{N} \sum_{\ell=1}^{L} R_\ell^{(i,0)} \left(F_{\gamma^{(i,0)}} \left(\frac{-1}{b} \ln \left(1 - R_{\ell-1}^{(i,0)} \right) \right) \right. \\ &\left. - F_{\gamma^{(i,0)}} \left(\frac{-1}{b} \ln \left(1 - R_\ell^{(i,0)} \right) \right) \right), \\ &\text{s.t. } 0 \leqslant R_\ell^{(i,0)} \leqslant R_{\ell-1}^{(i,0)} \leqslant 1 \text{ and } R_\ell^{(i,0)} = R_\ell^{(j,0)}, \\ &\quad i \neq j, i, j \in \mathcal{I}, \ell \in \mathcal{L}, \end{aligned} \tag{17}$$

$$\max \sum_{i=1}^{N} \sum_{\ell=1}^{L} \frac{1}{\ell} R^{(i,0)} \left(F_{\gamma^{(i,0)}} \left(\frac{-1}{b(\ell-1)} \ln(1 - R^{(i,0)}) \right) \right.$$

$$- F_{\gamma^{(i,0)}}\left(\frac{-1}{b\ell}\ln\left(1-R^{(i,0)}\right)\right)\Bigg),$$

$$\text{s.t. } 0 \leqslant R^{(i,0)} \leqslant 1 \text{ and } R^{(i,0)} = R^{(j,0)},$$
$$i \neq j, i, j \in \mathcal{I}, \tag{18}$$

where $F_{\gamma^{(i,0)}}(x)$ is the cumulative distribution function (CDF) of $\gamma^{(i,0)}$ which can be obtained as follows:

$$F_{\gamma^{(i,0)}}(x) = \int_0^{\infty}\left(f_{h_p^{(i,0)}}(h_p)\int_0^{\frac{\sigma n\sqrt{x}}{2\rho P_t h_p}} f_{h_t^{(i,0)}}(h_t)dh_t\right)dh_p, \tag{19}$$

where $f_{h_t^{(i,0)}}(h_t)$, and $f_{h_p^{(i,0)}}(h_p)$ are defined in (2) and (4), respectively. We will adopt a numerical method to solve (17) and (18) in Section IV.

2) HARQ With CIRP: We first derive expressions of the average sum rate for an FSO broadcasting setting in which a central node is serving two users under the CIRP; we then extend this analysis to the case of three users and finally discuss its extension to more than three users. It should be noted that we do not need to normalize the SNR with respect to the number of transmit apertures (i.e., two), since only one transmit aperture is effectively utilized during each retransmission round.

Two Users: Since two users are allowed to cooperate in the retransmission process, the average sum rate can be formulated by considering the following scenarios:

- Both users successfully decode the (re)transmitted packet from the central node at the ℓ^{th} round and hence, no communication occurs between the users. In this case, the sum rate is $(R_\ell^{(1,0)} + R_\ell^{(2,0)})$ and $(\frac{R^{(1,0)}}{\ell} + \frac{R^{(2,0)}}{\ell})$ for the IR and CC schemes, respectively.
- Both users successfully decodes the (re)transmitted packet. One user, for example the first user, successfully decodes the (re)transmitted packet at round ℓ_1 while the second user decodes it later at round ℓ_2, i.e., $\ell_2 > \ell_1$. From round ℓ_1 on, the retransmission process is switched from the central node to the first user who had declared its successful decoding at round ℓ_1. In this case, the sum rate is $(R_{\ell_1}^{(1,0)} + R_{\ell_2}^{(2,1)})$ and $(\frac{R^{(1,0)}}{\ell_1} + \frac{R^{(2,1)}}{\ell_2})$ for the IR and CC schemes, respectively.
- Only one user, for example the first user, successfully decodes the (re)transmitted packet at round ℓ and an error is declared by the other one. From round $(\ell+1)$ on, the retransmission procedure is switched from the central node to the first user who had declared its successful decoding at the ℓ^{th} (re)transmission round. In this case, the sum rate is $R_\ell^{(1,0)}$ and $\frac{R^{(1,0)}}{\ell}$ for the IR and CC schemes.
- No user can successfully decode the (re)transmitted packet and the sum rate is zero.

By taking into account the above scenarios as well as previous discussion for the traditional protocol, one can obtain the average sum rate for the CIRP with two users as for the IR and CC schemes, respectively. It should be noted that in the last two terms of (20) and (21) shown at the bottom of this page, the multiplying factors of $\pi_{(\infty,L)}^{(2,1)}$, $\pi_{(\infty,L)}^{(1,2)}$, $\kappa_{(L,\infty)}^{(2,1)}$, and $\kappa_{(L,\infty)}^{(1,2)}$ vanish at the L^{th} round since no retransmission occurs over the optical links between users. Similar to (14) and (15), the optimization problems for the maximum achievable sum rate

$$\begin{aligned}\overline{\Upsilon}_{\text{IR}} = &\sum_{\ell=1}^{L}\left(R_\ell^{(1,0)}+R_\ell^{(2,0)}\right)\pi_{(\ell,\ell-1)}^{(1,0)}\pi_{(\ell,\ell-1)}^{(2,0)}+\sum_{\ell_1=1}^{L-1}\sum_{\ell_2=\ell_1+1}^{L}\left(R_{\ell_1}^{(1,0)}+R_{\ell_2}^{(2,1)}\right)\pi_{(\ell_1,\ell_1-1)}^{(1,0)}\pi_{(\infty,\ell_1)}^{(2,0)}\times\{\pi_{(\ell_2,0)}^{(2,1)}\delta(\ell_2-\ell_1-1)\\
&+\pi_{(\ell_2,\ell_2-1)}^{(2,1)}u(\ell_2-\ell_1-2)\}+\sum_{\ell_2=1}^{L-1}\sum_{\ell_1=\ell_2+1}^{L}\left(R_{\ell_1}^{(1,2)}+R_{\ell_2}^{(2,0)}\right)\pi_{(\ell_2,\ell_2-1)}^{(2,0)}\pi_{(\infty,\ell_2)}^{(1,0)}\times\{\pi_{(\ell_1,0)}^{(1,2)}\delta(\ell_1-\ell_2-1)+\pi_{(\ell_1,\ell_1-1)}^{(1,2)}u(\ell_1-\ell_2-2)\}\\
&+\sum_{\ell=1}^{L}R_\ell^{(1,0)}\pi_{(\ell,\ell-1)}^{(1,0)}\pi_{(\infty,\ell)}^{(2,0)}[\pi_{(\infty,L)}^{(2,1)}u(L-\ell-1)+\delta(L-\ell)]+\sum_{\ell=1}^{L}R_\ell^{(2,0)}\pi_{(\ell,\ell-1)}^{(2,0)}\pi_{(\infty,\ell)}^{(1,0)}[\pi_{(\infty,L)}^{(1,2)}u(L-\ell-1)+\delta(L-\ell)].\end{aligned} \tag{20}$$

$$\begin{aligned}\overline{\Upsilon}_{\text{CC}} = &\sum_{\ell=1}^{L}\frac{1}{\ell}\left(R^{(1,0)}+R^{(2,0)}\right)\kappa_{(\ell-1,\ell)}^{(1,0)}\kappa_{(\ell-1,\ell)}^{(2,0)}+\sum_{\ell_1=1}^{L-1}\sum_{\ell_2=\ell_1+1}^{L}\left(\frac{1}{\ell_1}R^{(1,0)}+\frac{1}{\ell_2}R^{(2,1)}\right)\kappa_{(\ell_1-1,\ell_1)}^{(1,0)}\kappa_{(\ell_1,\infty)}^{(2,0)}\\
&\times\{\kappa_{(0,\ell_2)}^{(2,1)}\delta(\ell_2-\ell_1-1)+\kappa_{(\ell_2-1,\ell_2)}^{(2,1)}u(\ell_2-\ell_1-2)\}+\sum_{\ell_2=1}^{L-1}\sum_{\ell_1=\ell_2+1}^{L}\left(\frac{1}{\ell_1}R^{(1,2)}+\frac{1}{\ell_2}R^{(2,0)}\right)\kappa_{(\ell_2-1,\ell_2)}^{(2,0)}\kappa_{(\ell_2,\infty)}^{(1,0)}\\
&\times\{\kappa_{(0,\ell_1)}^{(1,2)}\delta(\ell_1-\ell_2-1)+\kappa_{(\ell_1-1,\ell_1)}^{(1,2)}u(\ell_1-\ell_2-2)\}+\sum_{\ell=1}^{L}\frac{1}{\ell}R^{(1,0)}\kappa_{(\ell-1,\ell)}^{(1,0)}\kappa_{(\ell,\infty)}^{(2,0)}[\kappa_{(L,\infty)}^{(2,1)}u(L-\ell-1)\\
&+\delta(L-\ell)]+\sum_{\ell=1}^{L}\frac{1}{\ell}R^{(2,0)}\kappa_{(\ell-1,\ell)}^{(2,0)}\kappa_{(\ell,\infty)}^{(1,0)}[\kappa_{(L,\infty)}^{(1,2)}u(L-\ell-1)+\delta(L-\ell)].\end{aligned} \tag{21}$$

TABLE I
SUM RATE WHEN THREE USERS SUCCESSFULLY DECODE

Rounds \ Scheme	IR	CC
$\ell_i=\ell_{t_i}=\ell_{t'_i}=\ell$	$R_\ell^{(i,0)}+R_\ell^{(t_i,0)}+R_\ell^{(t'_i,0)}$	$\frac{1}{\ell}\left(R^{(i,0)}+R^{(t_i,0)}+R^{(t'_i,0)}\right)$
$\ell_i=\ell_{t_i}<\ell_{t'_i}$	$R_{\ell_i}^{(i,0)}+R_{\ell_i}^{(t_i,0)}+R_{\ell_{t'_i}}^{(t'_i,t_i)}$	$\frac{R^{(i,0)}+R^{(t_i,0)}}{\ell_i}+\frac{R^{(t'_i,t_i)}}{\ell_{t'_i}}$
$\ell_i<\ell_{t_i}=\ell_{t'_i}$	$R_{\ell_i}^{(i,0)}+R_{\ell_{t_i}}^{(t_i,i)}+R_{\ell_{t_i}}^{(t'_i,0)}$	$\frac{R^{(i,0)}}{\ell_i}+\frac{R^{(t_i,i)}+R^{(t'_i,0)}}{\ell_{t_i}}$
$\ell_i<\ell_{t_i}<\ell_{t'_i}$	$R_{\ell_i}^{(i,0)}+R_{\ell_{t_i}}^{(t_i,i)}+R_{\ell_{t'_i}}^{(t'_i,t_i)}$	$\frac{R^{(i,0)}}{\ell_i}+\frac{R^{(t_i,i)}}{\ell_{t_i}}+\frac{R^{(t'_i,t_i)}}{\ell_{t'_i}}$
$\ell_i<\ell_{t'_i}<\ell_{t_i}$	$R_{\ell_i}^{(i,0)}+R_{\ell_{t_i}}^{(t_i,i)}+R_{\ell_{t_i}}^{(t'_i,0)}$	$\frac{R^{(i,0)}}{\ell_i}+\frac{R^{(t_i,i)}}{\ell_{t_i}}+\frac{R^{(t'_i,0)}}{\ell_{t'_i}}$

TABLE II
SUM RATE WHEN TWO USERS SUCCESSFULLY DECODE

Rounds \ Scheme	IR	CC
$\ell_i=\ell_{t_i}=\ell$	$R_\ell^{(i,0)}+R_\ell^{(t_i,0)}$	$\frac{1}{\ell}\left(R^{(i,0)}+R^{(t_i,0)}\right)$
$\ell_i=\ell_{t'_i}=\ell$	$R_\ell^{(i,0)}+R_\ell^{(t'_i,0)}$	$\frac{1}{\ell}\left(R^{(i,0)}+R^{(t'_i,0)}\right)$
$\ell_i<\ell_{t_i}$	$R_{\ell_i}^{(i,0)}+R_{\ell_{t_i}}^{(t_i,i)}$	$\frac{R^{(i,0)}}{\ell_i}+\frac{R^{(t_i,i)}}{\ell_{t_i}}$
$\ell_i<\ell_{t'_i}$	$R_{\ell_i}^{(i,0)}+R_{\ell_{t'_i}}^{(t'_i,0)}$	$\frac{R^{(i,0)}}{\ell_i}+\frac{R^{(t'_i,0)}}{\ell_{t'_i}}$

can be formulated as

$$\begin{aligned}&\max \overline{\Upsilon}_{\text{IR}},\\ &\text{s.t. } 0\leqslant R_\ell^{(i,0)}\leqslant R_{\ell-1}^{(i,0)}\leqslant 1, 0\leqslant R_\ell^{(i,j)}\leqslant R_{\ell-1}^{(i,j)}\leqslant 1,\\ &\quad R_\ell^{(i,j)}=R_\ell^{(j,i)}, \text{ and } R_\ell^{(i,0)}=R_\ell^{(j,0)},\\ &\quad i\neq j, i,j=1,2, \ell\in\mathcal{L},\end{aligned} \tag{22}$$

and

$$\begin{aligned}&\max \overline{\Upsilon}_{\text{CC}},\\ &\text{s.t. } 0\leqslant R^{(i,j)}, R^{(i,0)}\leqslant 1, R^{(i,j)}=R^{(j,i)}, \text{ and } R^{(i,0)}=R^{(j,0)},\\ &\quad i\neq j, i,j=1,2,\end{aligned} \tag{23}$$

for the IR and CC schemes, respectively.

Three Users: As the number of users increases by one, more possibilities should be considered for the average sum rate evaluation. For this case, we first number a possible sequence of users by three parameters i, t_i, and t'_i, where $t_i = \mod(i,3)+1$, $t'_i = \mod(i+1,3)+1$, and $i\in\{1,2,3\}$. Then, we consider the following scenarios:

- All three users successfully decode the (re)transmitted packet from the central node and/or from their neighboring users. Depending on which user(s) decodes earlier than the others, five different cases are observed:
  i) All three users decode at the ℓ^{th} round.
  ii) Two consecutive users decode at the ℓ_i^{th} round and the other decodes at the $\ell_{t'_i}^{th}$ round such that $\ell_i<\ell_{t'_i}$.
  iii) One user decodes at the ℓ_i^{th} round and the other two consecutive users decode at the $\ell_{t_i}^{th}$ round such that $\ell_i<\ell_{t_i}$.
  iv) Users decode in a circular sequence at the ℓ_i^{th}, $\ell_{t_i}^{th}$, and $\ell_{t'_i}^{th}$ rounds such that $\ell_i<\ell_{t_i}<\ell_{t'_i}$.
  v) Users decode in a non-ordered sequence at the end of ℓ_i^{th}, $\ell_{t_i}^{th}$, and $\ell_{t'_i}^{th}$ rounds such that $\ell_i<\ell_{t'_i}<\ell_{t_i}$.
  Table I lists the sum rates of these five cases for both IR and CC schemes.
- Two users successfully decode the (re)transmitted packet from the central node and/or from the users and the other one fails. Depending on which user(s) can decode earlier than the other ones, four different cases are observed:
  i) Two consecutive users decode at the ℓ^{th} (re)transmission round.
  ii) Two non-consecutive users decode at the ℓ^{th} round.
  iii) Two consecutive users decode at the ℓ_i^{th} and $\ell_{t_i}^{th}$ rounds such that $\ell_i<\ell_{t_i}$.
  iv) Two non-consecutive users decode at the ℓ_i^{th} and $\ell_{t'_i}^{th}$ rounds such that $\ell_i<\ell_{t'_i}$.
  Table II lists the sum rates of these four cases for both IR and CC schemes.
- Only one user can successfully decode the (re)transmitted packet from the central node at the ℓ_i^{th} round and the others fail. The sum rate is $R_{\ell_i}^{(i,0)}$ and $\frac{R^{(i,0)}}{\ell_i}$ for the IR and CC schemes, respectively.

Similar to (20) and (21) for the IR and CC schemes, the average sum rate formulas can be simply obtained by using the sum-rates expressions given in Tables I and II. Since the formulas of average sum rate are lengthy for both schemes, we omit their expressions here to simplify the presentation.

From the above examples for two and three users, it can be understood that finding a general formula for the average sum rate of CIRP is a cumbersome task. This difficulty arises because the number of possible events increases combinatorially with N. We believe that the guidelines provided by examples for $N=2$ and $N=3$ pave the way for the extension to larger number of users. However, we analyze the NRPS of both protocols from a more general perspective to demonstrate the superiority of the CIRP over the traditional protocol. To this end, we present the following theorem:

Theorem 1: Consider a homogeneous HARQ FSO broadcasting system in which the central node and users are communicating under the IR scheme. Assume that $N-n$ users have successfully decoded the transmitted packets by the end of the $(\ell-1)^{th}$ retransmission round where $1\leq n\leq N-1$ and $2\leq\ell\leq L$. For the ℓ^{th} round, we denote the NRPS for all remaining users under the traditional protocol and CIRP by $\mathcal{P}$ and $\tilde{\mathcal{P}}$, respectively. Moreover, $\pi_{(\ell,\ell-1)}$ and $\tilde{\pi}_{(\ell,\ell-1)}$ represent the LSPs of user $i\in\mathcal{N}=\{1,2,\ldots,n\}$ over the links $(i,0)$ and (i,j), respectively, and where j is the neighboring user of user i who has already successfully decoded the packet. Under the condition $\tilde{\pi}_{(\ell,\ell-1)}\geq\pi_{(\ell,\ell-1)}$, we have

$$\tilde{\mathcal{P}}\geq\mathcal{P}. \tag{24}$$

Proof: We start first with derivation of $\mathcal{P}$ and $\tilde{\mathcal{P}}$. Using the definition of LSP given in (8), the independency of links between the central node and different users, and the system homogeneity, $\mathcal{P}$ can be readily derived as follows:

$$\mathcal{P}=\left[\pi_{(\ell,\ell-1)}\right]^n. \tag{25}$$

In order to obtain $\tilde{\mathcal{P}}$, we define $p(n_1, n_2)$ corresponding to the probability of the event that n_1 out of n users do not have a neighboring user who has already and successfully decoded the packet while the rest, i.e., $n_2 \triangleq n - n_1$ have such a neighboring user. Now, we fix the value of n_1 and obtain the conditional probability $\tilde{\mathcal{P}}$ at the ℓ^{th} round as follows:

$$\left[\pi_{(\ell,\ell-1)}\right]^{n_1} \left[\tilde{\pi}_{(\ell,\ell-1)}\right]^{n_2}, \tag{26}$$

where we again assume the independency of different links and the system homogeneity. By using the well-known total probability theorem, probability $\tilde{\mathcal{P}}$ can be derived as follows:

$$\tilde{\mathcal{P}} = \sum_{(n_1,n_2)} p(n_1, n_2) \left[\pi_{(\ell,\ell-1)}\right]^{n_1} \left[\tilde{\pi}_{(\ell,\ell-1)}\right]^{n_2}. \tag{27}$$

Finally, (24) can be simply deduced by applying the condition $\tilde{\pi}_{(\ell,\ell-1)} \geq \pi_{(\ell,\ell-1)}$ and the fact that $\sum_{(n_1,n_2)} p(n_1, n_2) = 1$. ■

Remark 1: From Theorem 1, it can be concluded that the advantage of CIRP over the traditional protocol will be confirmed if the condition $\tilde{\pi}_{(\ell,\ell-1)} \geq \pi_{(\ell,\ell-1)}$ is observed. Unfortunately, a comparison between $\pi_{(\ell,\ell-1)}$ and $\tilde{\pi}_{(\ell,\ell-1)}$ based on a mathematical analysis of CDFs and LSPs is not feasible due to the following reasons: $i)$ a closed-form mathematical expression does not exist for the integral given in (19), $ii)$ even by deriving a closed-form expression for (19), we should finally resort to numerical analyses since the CDFs are functions of the SNR, visibility, and refractive index. In order to compare the LSPs $\pi_{(\ell,\ell-1)}$ and $\tilde{\pi}_{(\ell,\ell-1)}$, we have conducted a comprehensive numerical analysis in Section IV-A by varying various parameters. According to the discussions given in Section IV-A, the condition $\tilde{\pi}_{(\ell,\ell-1)} \geq \pi_{(\ell,\ell-1)}$ holds for a given pair $(R_{\ell-1}, R_\ell)$ at a high LSP. It is worthwhile to mention that imposing the LSP to be high for a pair $(R_{\ell-1}, R_\ell)$ guarantees a reliable communication over an FSO broadcasting link. Hence, it is not a limiting factor for observing the condition in Theorem 1 and the condition is easily satisfied in the practical scenarios.

Remark 2: A similar result can be obtained from the worst-case scenario analysis where $n_1 = n - 1$ and $n_2 = 1$ corresponding to the event that users who have successfully decoded the packet by the end of the $(\ell-1)^{th}$ round are consecutive and hence, the users who are requesting for the packet in the ℓ^{th} round follow the same ensuing pattern. [4] For this scenario, we can write

$$\tilde{\mathcal{P}}_{\text{worst}} = \left[\pi_{(\ell,\ell-1)}\right]^{n-1} \left[\tilde{\pi}_{(\ell,\ell-1)}\right] \geq \mathcal{P}, \tag{28}$$

for a given pair $(R_{\ell-1}, R_\ell)$ at a high LSP.

Remark 3: We note that $\tilde{\mathcal{P}} = \mathcal{P}$ when $n = N$ under any circumstances since in this case, (which is excluded from Theorem 1) no user has successfully decoded the packet by the end of the $(\ell-1)^{th}$ round, and the CIRP performs the same as traditional protocol. However, the probability of such an event is equal to

$$\left[1 - \pi_{(\ell,\ell-1)}\right]^N, \tag{29}$$

which goes rapidly to zero as ℓ increases (or equivalently as R_ℓ decreases) and/or if N is large. Hence, the probability of successful decoding by at least one user is very high at the early rounds when N is large. From the round in which at least one user could successfully decode the packet, the CIRP outperforms the traditional protocol since $\mathcal{P}_{\text{worst}} \geq \mathcal{P}$.

Remark 4: Theorem 1 can similarly be proven for the CC scheme by replacing $\pi_{(\ell,\ell-1)}$ and $\tilde{\pi}_{(\ell,\ell-1)}$ with $\kappa_{(\ell-1,\ell)}$ and $\tilde{\kappa}_{(\ell-1,\ell)}$, respectively. Then, the condition $\tilde{\kappa}_{(\ell,\ell-1)} \geq \kappa_{(\ell,\ell-1)}$ is similarly met for a given pair (R, ℓ) at a high LSP according to the discussions given in Section IV-A.

[4]Due to the homogeneity assumption, the whole system can be viewed as a circle with the central node as its center and the users distributed on its circumference. The interuser cooperation is assumed in either clockwise or counterclockwise direction.

TABLE III
SYSTEM SPECIFICATIONS

Parameters	Symbol	Value
Wavelength	λ	1550nm
Refractive index	C_n^2	$[10^{-15},\ 10^{-13}]\text{m}^{-2/3}$
Beam waist at $d = 0$	ω_0	2.5m
Jitter standard deviation	σ_{pe}	0.3m
Attenuation coefficient	ζ	3.3dB/km
Detector's radius	a	0.1m
Noise standard deviation	σ_n	10^{-7}
Photodetector's responsivity	ρ	0.5A/W

IV. NUMERICAL RESULTS

In this section, we first numerically compare the CDFs and LSPs of the links $(i, 0)$ and (i, j) as defined in Theorem 1, in order to support the observations made in Remarks 1–4 above. Then, we carry on numerical analysis to evaluate the average sum rate of the FSO broadcasting system which operates under an HARQ scheme. To this end, we use the exhaustive search to solve the optimization problems. Also, we use the built-in MATLAB function *trapz* to compute the integral in (19). We consider a homogeneous FSO broadcasting system with one central node and $N = 2$. The central node is equipped with two transmit apertures while each user utilizes one receive aperture for the traditional protocol, and one transmit and two receive apertures for the CIRP. The central node (and both users for the CIRP) utilize the OOK modulation scheme in the transmission and retransmission rounds. The maximum number of transmissions is assumed to be $L = 2$. The distance between the central node and each user is set to 5 km, while the nominal distance between the two users is varied between 0.5 km and 4 km. Other system specifications are listed in Table III. Note that we consider $C_n^2 = 2 \times 10^{-15}\ \text{m}^{-2/3}$ and $C_n^2 = 10^{-13}\ \text{m}^{-2/3}$ for the weak and strong turbulence, respectively. Also, the given value $\zeta = 3.3$ dB/km corresponds to the low visibility condition of 1 kilometer. Note that by taking into account the system homogeneity, the optimal solutions of problems (17) and (18) can be found by solving an equivalent problem for only one user.

A. Study of CDFs and LSPs of Links $(i, 0)$ and (i, j)

We denote the distance between the central node and a user by d and the distance between each pair of consecutive users by $\tilde{d}$, and provide the CDFs curves of link capacity for different

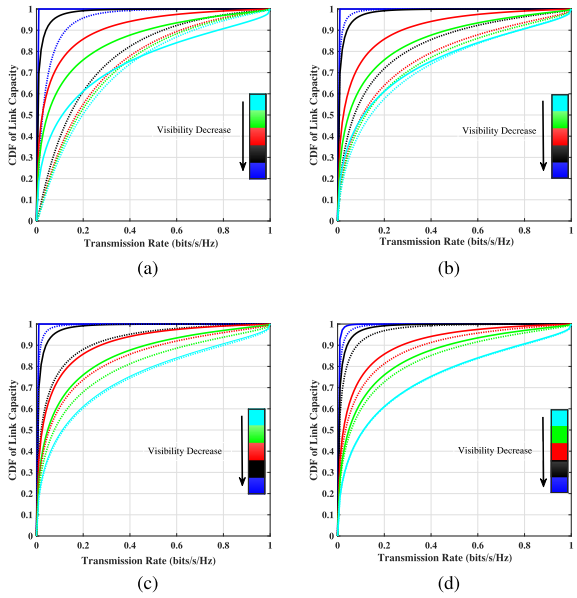

Fig. 3. CDFs of capacity for the links from the central node (solid lines) and neighboring user (dashed lines) to user i when the SNR is normalized, and the distance between the central node and all users is set to 5 km, and the distance between each pair of users is (a) 0.5 km, (b) 1 km, (c) 2.5 km, (d) 4 km, and for $C_n^2 = 10^{-13}$.

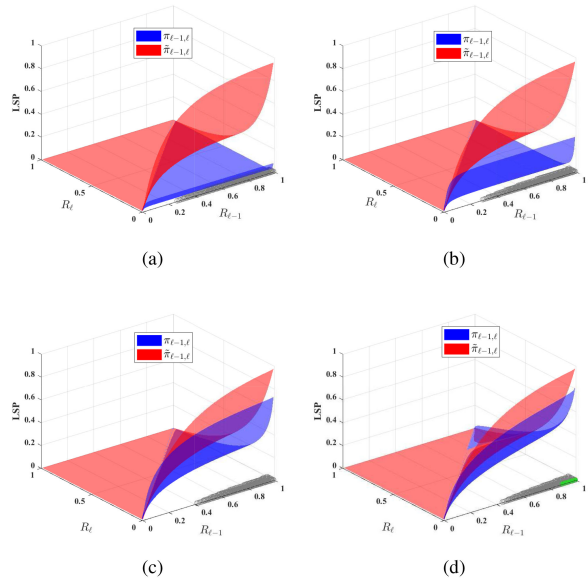

Fig. 4. LSPs of (i, j) and $(i, 0)$ under the IR scheme when the SNR is normalized and $\tilde{d}/d = 0.1$, and the visibility is (a) 3 km (thin fog), (b) 4 km (haze), (c) 10 km (light haze), (d) 51 km (clear). The gray and green shaded regions represent the areas where $\tilde{\pi}_{(\ell,\ell-1)} \geq 75\%$ and $\pi_{(\ell,\ell-1)} \geq 75\%$, respectively, and for $C_n^2 = 10^{-13}$.

values of $\tilde{d}$ and visibility conditions in Fig. 3. Note that the SNR is normalized with respect to the parameter $2(\frac{\rho P_t}{\sigma_n})^2$ while the effect of pointing errors is not considered in Fig. 3. As seen from the figure, the 80%-likely capacity achieved by the link (i, j) outperforms that of the link $(i, 0)$ over various visibility conditions apart from the case where $\tilde{d}/d = 0.8$ under high visibility. Moreover, the median capacity provided by the link $(i, 0)$ is slightly greater than that of the link (i, j) for the case where $\tilde{d}/d = 0.1$ under high visibility (see Fig. 1a), while it does not hold true as $\tilde{d}$ increases. Hence, we could observe that the capacity achieved by the link (i, j) is greater than that of the link $(i, 0)$ in most scenarios especially when the visibility is low. Although the link capacity is the ultimate performance metric of a communication system, we will discuss the LSP superiority of (i, j) over $(i, 0)$ in the following.

Next, we compare the LSPs $\pi_{(\ell,\ell-1)}$ and $\tilde{\pi}_{(\ell,\ell-1)}$ versus $(R_{\ell-1}, R_\ell)$ in Fig. 4 for the case where $\tilde{d}/d = 0.1$ in various visibility situations. As seen from the figure, no point is included within the green region, where $\pi_{(\ell,\ell-1)} \geq 75\%$, under poor visibility condition (see Figs. 2a-2c), while the gray region, where $\tilde{\pi}_{(\ell,\ell-1)} \geq 75\%$, is relatively wide at the same visibility condition. As the visibility condition improves, both regions will become wider, while the green region involves points at low values of R_ℓ (see Fig. 4d). Hence, for a high LSP, there exists a pair of $(R_{\ell-1}, R_\ell)$ over the link (i, j) whose R_ℓ is greater than that of the link $(i, 0)$. Moreover, it can be observed that $\tilde{\pi}_{(\ell,\ell-1)} \geq \pi_{(\ell,\ell-1)}$ over the green region where $\pi_{(\ell,\ell-1)} \geq 75\%$.

We also depict $\kappa_{(\ell-1,\ell)}$ and $\tilde{\kappa}_{(\ell-1,\ell)}$ versus R and ℓ in Fig. 5 for the CC scheme. As seen from this figure, similar results to those of the IR scheme can be deduced for the CC scheme. It should be emphasized that Figs. 4 and 5 are obtained under the strong turbulence condition when $C_n^2 = 10^{-13}$. However,

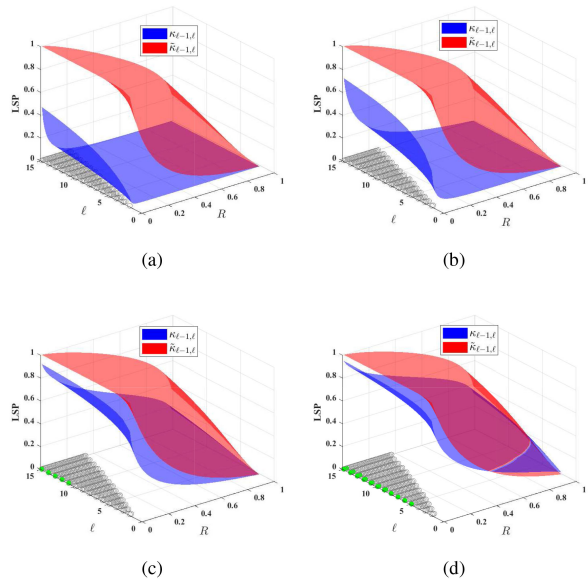

Fig. 5. LSPs of (i, j) and $(i, 0)$ under the CC scheme when the SNR is normalized and $\tilde{d}/d = 0.1$, and the visibility is (a) 3 km (thin fog), (b) 4 km (haze), (c) 10 km (light haze), (d) 51 km (clear). The gray and green shaded regions represent the areas where $\tilde{\kappa}_{(\ell-1,\ell)} \geq 90\%$ and $\kappa_{(\ell-1,\ell)} \geq 90\%$, respectively, and for $C_n^2 = 10^{-13}$.

similar curves can be obtained when the turbulence condition is weak. We have not presented here these extra results due to the space limitation.

B. Average Sum Rate Optimization

Fig. 6 depicts the maximum achievable average sum rate versus P_t for an FSO broadcasting system which operates under the IR scheme. Here, we fix the distance between the two users to be $\tilde{d} = 1$ km. As seen from the figure, the CIRP outperforms

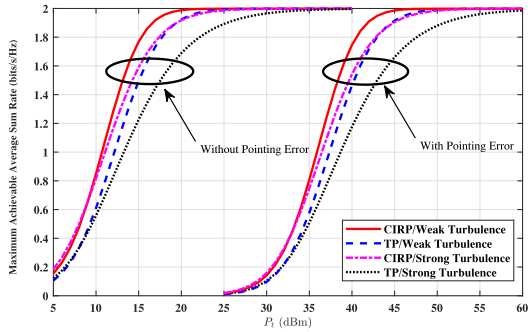

Fig. 6. Maximum average transmission rates versus P_t for traditional and CIRP protocols with IR scheme under different turbulence conditions (TP stands for Traditional Protocol).

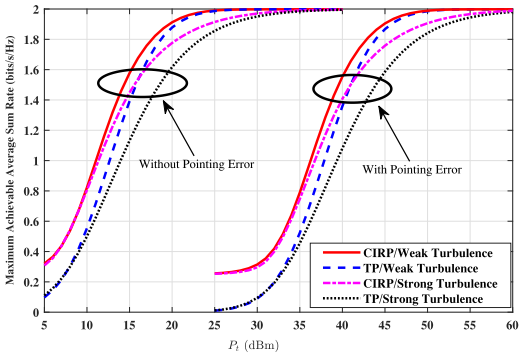

Fig. 7. Maximum average transmission rates versus P_t for traditional and CIRP protocols with CC scheme under different turbulence conditions.

the traditional protocol for a wide range of turbulence conditions whether random pointing errors exist or not. For example, when there is no random pointing errors under weak and strong turbulence conditions, the maximum achievable sum rates at $P_t = 15$ dBm are 1.8 and 1.6 bits/s/Hz for the CIRP while they are 1.5 and 1.2 bits/s/Hz for the traditional protocol, respectively. The CIRP still has this advantage of sum rate over the traditional protocol when the random pointing errors exist.

The maximum achievable average sum rate versus P_t is illustrated in Fig. 7 where the system works under the CC scheme. Similar to the IR case, an analogous gain of average sum rate is provided by the CIRP in all range of P_t. As observed from the figure, the gap between the CIRP and the traditional protocol is wider in lower values of P_t. For instance, when there is random pointing errors under weak and strong turbulence conditions, the maximum achievable sum rates at $P_t = 30$ dBm are 0.314 and 0.296 bits/s/Hz for the CIRP, while they are 0.090 and 0.095 bits/s/Hz for the traditional protocol, respectively.

Several interesting observations can be made from Figs. 6 and 7: i) The gap between the maximum achievable average sum rates of CIRP and the traditional protocol is larger when the turbulence is strong. This implies that the distance has more effect on the average sum rate when the turbulence is strong and the proposed CIRP can compensate for it. ii) For low to moderate values of P_t, the CIRP under the strong turbulence condition outperforms the traditional protocol under the weak turbulence condition. This result stems from the fact that the system performance is approximately independent of the turbulence conditions in low values of P_t and the difference gradually

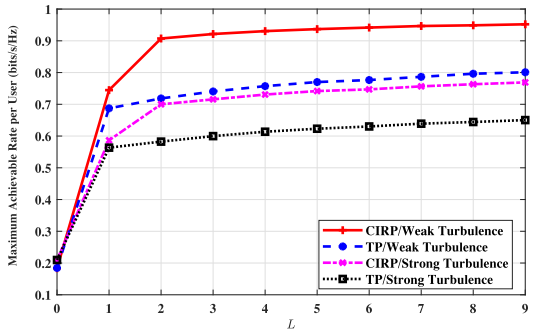

Fig. 8. Average successful transmission rate per user versus L for the traditional and CIRP protocols with IR scheme under different turbulence conditions without random pointing errors, and $P_t/h_o = -30$ (dBm).

becomes more pronounced as P_t increases. iii) The CIRP achieves a higher sum rate when the system works under the CC scheme compared to the IR scheme in low values of P_t. This result can be explained by observing how the traditional protocol can be extended to the CIRP. Under the traditional protocol, the achievable sum rates of IR and CC schemes are approximately the same in low values of P_t. When the CIRP is utilized, the rates of the interuser optical links, i.e., $R_2^{(1,2)}$ and $R^{(1,2)}$ for the IR and CC schemes, respectively, become additional degrees of freedom in the optimization. Since $0 \leqslant R_2^{(1,2)} \leqslant R_2^{(1,0)} \leqslant 1$ and $0 \leqslant R^{(1,2)} \leqslant 1$ in (22) and (23), respectively, $R_2^{(1,2)}$ is optimized over a limited range comparing to $R^{(1,2)}$. Hence, a lower average sum rate is achieved by the IR scheme. Note that if the retransmission process restarts over the intersuser optical links in the IR scheme, one more degree of freedom will be provided. This leads to an improved system performance for low values of P_t at the cost of more complexity.

Now, we investigate the effect of L on the average rate of successful transmission of a user for both protocols. To this end, we consider an HARQ system which works under the IR scheme in which the transmission rate is reduced by 10% if an unsuccessful decoding occurs. For this setup, Fig. 8 depicts the average successful transmission rate per user versus L for the traditional and CIRP protocols. The optical (re)transmission power is normalized by h_o (path loss) so as to consider merely the effect of scintillation index. As seen from the figure, the average success rate of the CIRP is significantly higher than that of the traditional protocol under various turbulence conditions. For example at $L = 4$, the average success rates under the weak and strong turbulence conditions are 0.93 and 0.73 bits/s/Hz for the CIRP, while the corresponding rates are 0.76 and 0.61 bits/s/Hz for the traditional protocol.

V. Conclusion

In this work, we proposed the HARQ CIRP for broadcasting systems over FSO channels, which is applicable to both IR and CC schemes. In contrast to the traditional transmission protocol, in the CIRP, optical users cooperate in the ARQ process. In particular, instead of relying on the central node, a user who successfully decoded the original data packet and whose distance from the NACK issuing user is smaller than that of the central node, is invited to retransmit this packet to the latter user.

We analyzed the performance of CIRP and traditional protocol from an information-theoretic point of view. Specifically, we formulated the maximum achievable sum rates problem and derived the NRPS expression for both protocols. Numerical results showed that the maximum achievable sum rates by the CIRP are higher than those of the traditional protocol under various turbulence conditions with and without random pointing errors.

REFERENCES

[1] A. G. Bell, "On the production and reproduction of sound by light," *Amer. J. Sci.*, vol. 20, no. 118, pp. 305–324, Oct. 1880.

[2] D. Kedar and S. Arnon, "Urban optical wireless communication networks: The main challenges and possible solutions," *IEEE Commun. Mag.*, vol. 42, no. 5, pp. 2–7, May 2004.

[3] M. Eghbal and J. Abouei, "Security enhancement in free-space optics using acousto-optic deflectors," *IEEE/OSA J. Opt. Commun. Netw.*, vol. 6, no. 8, pp. 684–694, Aug. 2014.

[4] M. A. Amirabadi and V. Tabataba Vakili, "A new optimization problem in FSO communication system," *IEEE Commun. Lett.*, vol. 22, no. 7, pp. 1442–1445, Jul. 2018.

[5] L. Li *et al.*, "Free-space optical communication using coherent detection and double adaptive detection thresholds," *IEEE Photon. J.*, vol. 11, no. 1, pp. 1–17, Feb. 2019.

[6] M. Eghbal and J. Abouei, "Performance improvement of MIMO FSO systems against destructive interference," *IET Commun.*, vol. 13, no. 18, pp. 2923–2931, Nov. 2019.

[7] R. M. Gagliardi and S. Karp, *Optical Communications*. Hoboken, NJ, USA: Wiley, New York, 1995.

[8] A. A. Farid and S. Hranilovic, "Outage capacity optimization for free-space optical links with pointing errors," *J. Lightw. Technol.*, vol. 25, no. 7, pp. 1702–1710, Jul. 2007.

[9] S. M. Navidpour, M. Uysal, and M. Kavehrad, "BER performance of free-space optical transmission with spatial diversity," *IEEE Trans. Wireless Commun.*, vol. 6, no. 8, pp. 2813–2819, Aug. 2007.

[10] S. M. Aghajanzadeh and M. Uysal, "Diversity-multiplexing trade-off in coherent free-space optical systems with multiple receivers," *IEEE/OSA J. Opt. Commun. Netw.*, vol. 2, no. 12, pp. 1087–1094, Dec. 2010.

[11] C. Abou-Rjeily and S. Haddad, "Cooperative FSO systems: Performance analysis and optimal power allocation," *J. Lightw. Technol.*, vol. 29, no. 7, pp. 1058–1065, Apr. 2011.

[12] L. Yang, X. Gao, and M.-S. Alouini, "Performance analysis of free-space optical communication systems with multiuser diversity over atmospheric turbulence channels," *IEEE Photon. J.*, vol. 6, no. 2, pp. 1–17, Apr. 2014.

[13] P. Puri, P. Garg, and M. Aggarwal, "Multiple user pair scheduling in TWR assisted FSO systems," *IEEE/OSA J. Opt. Commun. Netw.*, vol. 8, no. 5, pp. 290–301, May 2016.

[14] C. Kose and T. R. Halford, "Incremental redundancy hybrid ARQ protocol design for FSO links," in *Proc. Mil. Commun. Conf.*, Boston, MA, USA, Oct. 2009, pp. 1–7.

[15] A. R. Hammons and F. Davidson, "On the design of automatic repeat request protocols for turbulent free-space optical links," in *Proc. Mil. Commun. Conf.*, San Jose, CA, USA, Oct. 2010, pp. 808–813.

[16] K. Kiasaleh, "Hybrid ARQ for FSO communications through turbulent atmosphere," *IEEE Commun. Lett.*, vol. 14, no. 9, pp. 866–868, Oct. 2010.

[17] S. M. Aghajanzadeh and M. Uysal, "Information theoretic analysis of hybrid-ARQ protocols in coherent free-space optical systems," *IEEE Trans. Commun.*, vol. 60, no. 5, pp. 1432–1442, May 2012.

[18] V. V. Mai and A. T. Pham, "Performance analysis of cooperative-ARQ schemes in free-space optical communications," *IEICE Trans. Commun.*, vol. E97-B, no. 8, pp. 1614–1622, Aug. 2014.

[19] E. Zedini, A. Chelli, and M.-S. Alouini, "On the performance analysis of hybrid-ARQ with incremental redundancy and with code combining over free-space optical channels with pointing errors," *IEEE Photon. J.*, vol. 6, no. 4, pp. 1–18, Aug. 2014.

[20] S. S. Hosseini, J. Abouei, and M. Uysal, "Fast-decodable MIMO HARQ systems," *IEEE Trans. Wireless Commun.*, vol. 14, no. 5, pp. 2827–2840, May 2015.

[21] S. Sesia, G. Caire, and G. Vivier, "Incremental redundancy hybrid ARQ schemes based on low-density parity-check codes," *IEEE Trans. Commun.*, vol. 52, no. 8, pp. 1311–1321, Aug. 2004.

[22] D. Chase, "Code combining-A maximum-likelihood decoding approach for combining an arbitrary number of noisy packets," *IEEE Trans. Commun.*, vol. 33, no. 5, pp. 385–393, May 1985.

[23] J. Fang *et al.*, "Polar-coded MIMO FSO communication system over gamma-gamma turbulence channel with spatially correlated fading," *IEEE/OSA J. Opt. Commun. Netw.*, vol. 10, no. 11, pp. 915–923, Nov. 2018.

[24] J. Abouei and K. N. Plataniotis, "Multiuser diversity scheduling in free-space optical communications," *J. Lightw. Technol.*, vol. 30, no. 9, pp. 1351–1358, May 2012.

[25] J. Abouei, S. S. Hosseini, and K. N. Plataniotis, *Multiuser Diversity Scheduling: A New Perspective on the Future Development of FSO Communications*. Berlin, Germany: Springer, 2016, ch. 24, pp. 527–545.

[26] Y. F. Al-Eryani, A. M. Salhab, S. A. Zummo, and M. Alouini, "Two-way multiuser mixed RF/FSO relaying: Performance analysis and power allocation," *IEEE/OSA J. Opt. Commun. Netw.*, vol. 10, no. 4, pp. 396–408, Apr. 2018.

[27] Y. F. Al-Eryani, A. M. Salhab, S. A. Zummo, and M. Alouini, "Protocol design and performance analysis of multiuser mixed RF and hybrid FSO/RF relaying with buffers," *IEEE/OSA J. Opt. Commun. Netw.*, vol. 10, no. 4, pp. 309–321, Apr. 2018.

[28] L. Yang, M. O. Hasna, and I. S. Ansari, "Unified performance analysis for multiuser mixed η - μ and $\mathcal{M}$-distribution dual-hop RF/FSO systems," *IEEE Trans. Commun.*, vol. 65, no. 8, pp. 3601–3613, Aug. 2017.

[29] L. Chen, W. Wang, and C. Zhang, "Multiuser diversity over parallel and hybrid FSO/RF links and its performance analysis," *IEEE Photon. J.*, vol. 8, no. 3, pp. 1–9, Jun. 2016.

[30] C. B. Naila, K. Wakamori, M. Matsumoto, A. Bekkali, and K. Tsukamoto, "Transmission analysis of digital TV signals over a radio-on-FSO channel," *IEEE Commun. Mag.*, vol. 50, no. 8, pp. 137–144, Aug. 2012.

[31] Z. Nazari, A. Gholami, Z. Vali, M. Sedghi, and Z. Ghassemlooy, "Experimental investigation of scintillation effect on FSO channel," in *Proc. 24th Iranian Conf. Elect. Eng.*, Shiraz, Iran, May 2016, pp. 1629–1633.

[32] Z. Zhao, R. Liao, S. D. Lyke, and M. C. Roggemann, "Reed-Solomon coding for free-space optical communications through turbulent atmosphere," in *Proc. IEEE Aerosp. Conf.*, Mar. 2010, pp. 1–12.

[33] C. Shen and P. Fitz, "Hybrid ARQ in multiple-antenna slow fading channels: Performance limits and optimal linear dispersion code design," *IEEE Trans. Inf. Theory*, vol. 57, no. 9, pp. 5863–5883, Sep. 2011.

[34] M. Safari and M. Uysal, "Relay-assisted free-space optical communication," *IEEE Trans. Wireless Commun.*, vol. 7, no. 12, pp. 5441–5449, Dec. 2008.

[35] X. Zhu and J. M. Kahn, "Free-space optical communication through atmospheric turbulence channels," *IEEE Trans. Commun.*, vol. 50, no. 8, pp. 1293–1300, Aug. 2002.

[36] M. S. Awan, Marzuki, E. Leitgeb, B. Hillbrand, F. Nadeem, and M. S. Khan, "Cloud attenuations for free-space optical links," in *Proc. Int. Workshop Satell. Space Commun.*, Tuscany, Italy, Sep. 2009, pp. 274–278.

[37] S. M. Haas, "Capacity of and coding for multiple-aperture, wireless, optical communications," Ph.D. dissertation, Massachusetts Inst. Technol., Cambridge, Massachusetts, USA, May 2003.

[38] L. C. Andrews and R. L. Phillips, *Laser Beam Propagation Through Random Media*, 2nd ed. Bellingham, WA: SPIE Press, 2005.

[39] L. Yang, X. Gao, and M.-S. Alouini, "Performance analysis of relay-assisted all-optical FSO networks over strong atmospheric turbulence channels with pointing errors," *J. Lightw. Technol.*, vol. 32, no. 23, pp. 4011–4018, Dec. 2014.

[40] L. Andrews, R. Phillips, and C. Hopen, *Laser Beam Scintillation with Applications*. Bellingham, WA: SPIE Press, 2001.

[41] C. Shen, T. Liu, and M. Fitz, "On the average rate performance of Hybrid-ARQ in quasi-static fading channels," *IEEE Trans. Commun.*, vol. 57, no. 11, pp. 3339–3352, Nov. 2009.

[42] E. Baccarelli, "Asymptotically tight bounds on the capacity and outage probability for QAM transmissions over Rayleigh-faded data channels with CSI," *IEEE Trans. Commun.*, vol. 47, no. 9, pp. 1273–1277, Sep. 1999.

[43] S. B. Slimane, "Approximation to the symmetric capacity of Rayleigh fading channels with multi-level signals," *IEEE Commun. Lett.*, vol. 10, no. 3, pp. 129–131, Mar. 2006.

[44] W. Li, H. Yang, and D. Yang, "Simple approximation formula for the symmetric capacity," in *Proc. 3rd Int. Conf. Wireless Mobile Commun.*, Gosier, France, March 2007, pp. 30–33.